

A Novel Nitrogen-containing Glyceride from Fungal Saprobe *Tubeufia rubra* Reverses MDR of Tumor Cell Lines to Doxorubicin

Xuebo Zeng ^{1,2}, Shengyan Qian ^{2,3}, Yongzhong Lu ⁴, Yongjie Li ²
Lizhuang Chen ², Yixin Qian ², Zhangjiang He ^{2*} and Jichuan Kang ^{2*}

¹ School of Pharmaceutical Sciences, Guizhou University, Guiyang, Guizhou 550025, P. R. China

² Engineering and Research Center for Southwest Bio-Pharmaceutical Resources of National Education
Ministry of China, Guizhou University, Guiyang, Guizhou 550025, P. R. China

³ School of Life Science, Guizhou University, Guiyang, Guizhou 550025, P. R. China

⁴ School of Food and Pharmaceutical Engineering, Guizhou Institute of Technology, Guiyang, Guizhou
550003, P. R. China

(Received January 27, 2022; Revised March 08, 2022; Accepted April 12, 2022)

Abstract: A chemical investigation of secondary metabolites from the saprobic fungus *Tubeufia rubra* led to isolation of a novel nitrogen-containing glyceride, Rubracin A (**1**), and a novel eight-membered cyclic ether carboxylate methyl ester, Rubracin H (**2**). Together with six known compounds (**3-8**). The chemical structure of these new compounds were elucidated by 1D and 2D NMR and HR-ESI-MS techniques. Although, there are no observed cytotoxic effects of compound **1** against MCF-7/Dox A549/Dox, and K562/Dox cells at concentrations below 25 µg/mL, usage of compound **1** and doxorubicin revealed the MDR reversal via decreased IC₅₀ values than that of sole doxorubicin application in the cell lines. A preliminary Western Blot assay indicated that the MDR reversal of compound **1** was due to suppression of P-glycoprotein (P-gp) expression.

Keywords: Rubracin A; *Tubeufia rubra* PF02-2; cytotoxic activity; MDR reversal. © 2022 ACG Publications. All rights reserved.

1. Introduction

Cancer is regarded as one of the most serious diseases [1-2]. The common treatments used in the clinic include surgical resection, radiotherapy, and chemotherapy. Chemotherapy remains a key treatment method for different stages and many types of cancer [3]. However, resistance to antitumor drugs is a major problem in cancer chemotherapy. One of the principal mechanisms by which many cancers develop multidrug resistance (MDR) is upregulation of the P-glycoprotein (P-gp) expression [4]. It's an ATP-binding cassette (ABC) transporter with a broad-specificity transmembrane efflux pump that lowers intracellular concentrations of a wide range of medicines below the effective cytotoxic threshold [5-6]. Therefore, the high expression of P-gp has become an impediment to successful

* Corresponding authors: E-Mail: jckang@gzu.edu.cn (J.Kang) ; Phone:0851-88298675; Fax: 0851-88297499
zjhe3@gzu.edu.cn (Z. He)

chemotherapy, and it is very important to find new drugs or new reversal agents combined with cytotoxic drugs to overcome the MDR of tumor cells.

Microorganisms are a rich source of structurally intriguing and biologically active secondary metabolites [7-12]. Historically, microorganisms have been served as significant sources for drug leads [13-15]. In our search for reversal agents from natural products, a saprophytic fungus, *T. rubra*, was isolated from the decaying wood [16-20]. Further literature investigation revealed that the family has a wide variety of biological activities, including antibacterial [21-22], antitumor [23], and hypoglycemic activities [24]. Our previous study exhibited that the crude extract of *T. rubra* PF02-2 can reverse the multidrug resistance of MCF-7/Dox in vitro [25]. Herein, we report the isolation and structure elucidation of one new nitrogen-containing glyceride (**1**) and a novel eight-membered cyclic ether carboxylate methyl ester (**2**) analogue from *T. rubra* PF02-2 (Figure 1), together with six known compounds (**3-8**). We also report the biological activity of compound **1**.

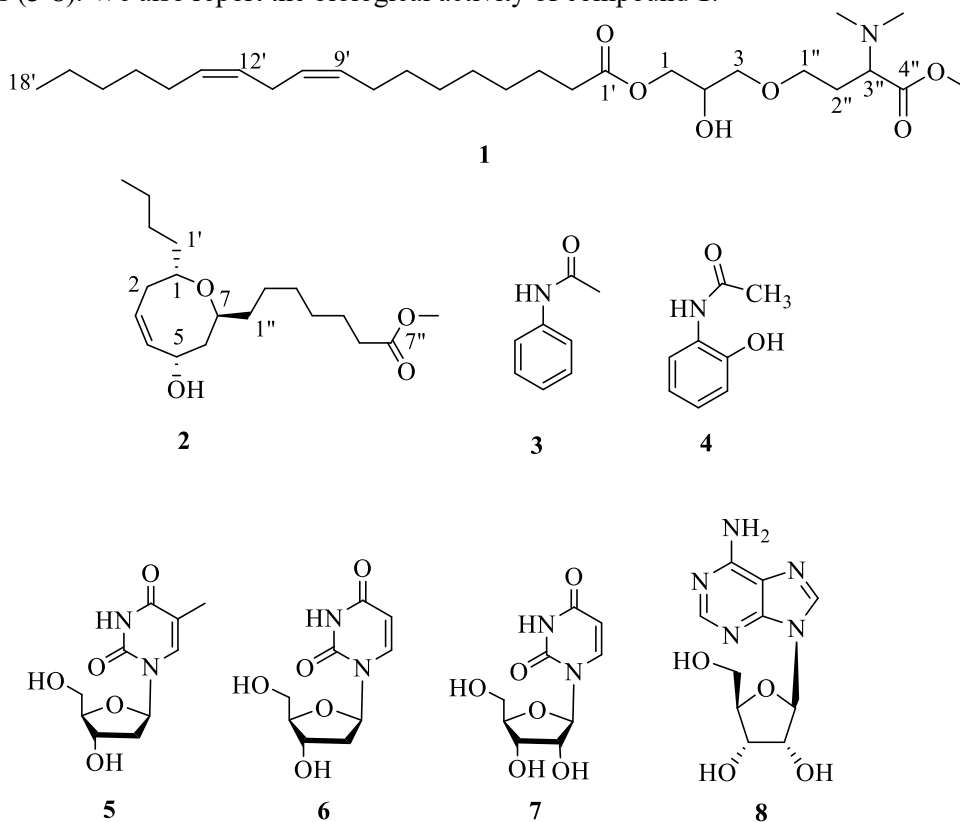


Figure 1. Structures of nitrogen constituents from *Tubeufia rubra* PF02-2

2. Materials and Methods

2.1. General Experimental Procedures

1D and 2D NMR spectra were recorded on a Bruker Avance III 500 MHz spectrometer with TMS as internal standard. High-resolution mass spectra were measured by using an Agilent G6230 time-of-flight mass spectrometer. The mass spectrometry data for the fragment ions were obtained on a Waters Auto Spec Premier P776 mass spectrometer. IR spectra were measured on a Thermo model Nicolet iS10 spectrometer using KBr pellets. UV spectra were obtained on a Shimadzu UV2401PC spectrometer. ECD spectra were performed on a Chirascan (v470.194) spectropolarimeter. ECD spectra were calculated via TDDFT at the B3LYP/def2-TZVP(-f) level. The calculated ECD spectrum of each conformer was generated with a bandwidth $\sigma = 0.3$ eV. The specific rotation was measured in Jasco P-1020 automatic digital polarimeter. C18-functionalized silica gel (40–63 μ m) was purchased from Merk Co., Ltd. Semipreparative HPLC separations were performed on a Tauto TBD2000 system equipped with a FUJI Chromatorex C18 column (20-45 μ m, 49 \times 460 mm). Silica gel (100–200 and 200–300

mesh) and Thin-layer chromatography (TLC) silica gel plates (GF254) were purchased from Qingdao Puke Separation Materials Co., Ltd. Cell Counting Kit-8 (CCK-8) was purchased from Shanghai Saint-Bio Biotechnology Co., Ltd. Cell lines for MCF-7/Dox (MXC230), MCF-7 (MXC231), A549/Dox (MXC779), A549 (MXC026), K562/Dox (MXC199), and K562 (MXC198) were purchased from Shanghai Meixuan Biotechnology Co., Ltd. BCA protein assay kit was purchased from Beyotime Biotechnology Co., Ltd. The ECL detection kit was purchased from Millipore.

2.2. Fungal Materials

T. rubra PF02-2 was obtained from decaying wood, which was collected in Fangchenggang City, Guangxi Province, China, in May 2016. The fungal strain was deposited at the China Center for Type Culture Collection (Wuhan) as CCTCC M2019957. *T. rubra* was cultivated on potato dextrose agar medium (PDA) at 28°C for 7 days. A 250 mL flask containing 100 mL of seed medium (PDB) was inoculated with chunks of agar with a well-grown culture of *T. rubra* and shaken on a rotary shaker at 28°C (at 180 rpm) for 3 days. The seed cultures were used to inoculate the production-scale fermentation. Each seed culture was transferred to a 1 L flask containing 200 g of oat and 150 mL of distilled water for 105 days.

2.3. Isolation and Purification

The fermented media was extracted with ethyl acetate (EtOAc) three times, and the solvent was removed under vacuum to obtain the EtOAc extract (201 g). The EtOAc extract was passed through a CH₂Cl₂–EtOAc system to obtain two components (E:35.77g and A:136g). The extract (E) was subjected to the RP-18 column and was separated by a linear gradient of H₂O/MeOH (90:10, 80:20, 70:30, 60:40, 50:50, 40:60, 30:70, 20:80, 10:90, and 0:100 v/v) to yield fourteen fractions (E1–E14). E11 (8.7 g) was separated by the RP-18 column, using the 30–100% MeOH–H₂O solvent to give twelve fractions (E11a–E11l). E11f (206 mg) was subjected to a silica gel column chromatography by eluting with CH₂Cl₂–MeOH (1:1 v/v) to afford three subfractions (E11fA–E11fC). E11fA (35 mg) was fractionated by a silica gel column with EtOAc–MeOH (1:1) to afford compound **1** (10 mg). E4 (7.01 g) was separated by the RP-18 column, using the 30–100% MeOH–H₂O solvent to give ten fractions (E4a–E4j). E4f (124 mg) was subjected to a silica gel column by eluting with CH₂Cl₂–EtOAc (25:1) to afford compound **3** (77 mg). E4b (116 mg) was subjected to a silica gel column by eluting with CH₂Cl₂–EtOAc (20:1) to afford two subfractions (E4bA–E4bB). E4bB (6.5 mg) was performed by Sephadex LH-20 column eluted with CH₂Cl₂–MeOH (1:1), producing compound **4** (2.5 mg). E4c (363 mg) was subjected to a silica gel column by eluting with CH₂Cl₂–EtOAc (20:1) to afford compounds **5** (5.2 mg) and **6** (6.5 mg). E4e (132 mg) was subjected to a silica gel column by eluting with CH₂Cl₂–EtOAc (10:1) to afford compounds **7** (4.1 mg) and **8** (10.3 mg).

The extract (A) was subjected to a silica gel column chromatography and was separated by a linear gradient of CH₂Cl₂/CH₃COCH₃ (100:1, 90:10, 80:20, 70:30, 60:40, 50:50, 40:60, 30:70, 20:80, 10:90, and 0:100) to yield 27 fractions (A1–A27). A6 (12.2 g) was separated by the RP-18 column, using the 60–100% MeOH–H₂O solvent to give 16 fractions (A6a–A6p). A6c (105 mg) was fractionated by a silica gel column with CH₂Cl₂–EtOAc (250:2) to afford compound **2** (5.3 mg).

Compound 1: Colorless oil; $[\alpha]_D^{29.1} = +14.2$ ($c=0.120$, CH₃OH); UV (MeOH) λ_{\max} (log ϵ) 196.5 (4.06) and 230 (3.49) nm; IR (KBr) ν_{\max} 3427, 2926, 2855, 1735, 1626, 1488, 1418, 1240, 1120 cm⁻¹; ¹H (500 MHz) and ¹³C NMR (125 MHz), see table 1 (CD₃OD); HRESIMS m/z 520.3611 [M + Na]⁺ (calcd. for C₂₈H₅₁NO₆Na, 520.3614).

Compound 2: Yellow oil; $[\alpha]_D^{18.4} = -85.06$ ($c=0.10$, CH₃OH); UV (MeOH) λ_{\max} (log ϵ) 203.0(3.80) and 226.5 (3.51) nm; IR (KBr) ν_{\max} 3443, 2931, 2859, 1740, 1633, 1545, 1437, 1254, 1172 cm⁻¹; ¹H (500 MHz) and ¹³C NMR (125 MHz), see table 2 (CD₃COCD₃); HR-ESIMS m/z 349.2349 [M + Na]⁺ (calcd. for C₁₉H₃₄O₄Na, 349.2336).

2.4. Cytotoxicity and MDR Reversal Activity Assays

MCF-7/Dox, A549/Dox, and K562/Dox cells were purchased from Shanghai MEIXUAN Biological Science and Technology Co., Ltd (Shanghai, China). The cytotoxicity of compound **1** against MCF-7/Dox, A549/Dox, and K562/Dox was tested using the CCK-8 assay [26]. The three cell lines were cultured in RPMI-1640 culture medium with 10% fetal bovine serum (FBS) at 37°C in a humidified atmosphere of 5% CO₂. The cells were seeded at a density of 2×10⁴ cells/well in 96-well plates and incubated for 24 h. Different concentrations of the positive control doxorubicin and the test compound **1** were subsequently added and incubated for 48 h. After the addition of 10 μL of CCK-8 to each well, the plate was incubated for 3 h under the same conditions to stain live cells. The absorbance in the control and drug-treated wells were measured by an enzyme-labeled instrument using a wavelength of 490 nm. All of the experiments were done in triplicate and twice. The cytotoxicity was expressed as IC₅₀ values (50% inhibitory concentration).

The MDR reversal activity of compound **1** was tested by the same method. Different concentrations of doxorubicin were added into wells in the presence or absence of compound **1** (5, 10, and 20 μg/mL) or verapamil (5, 10, and 20 μg/mL), which were then seeded with cells, respectively, after 48 h for the CCK-8 assay. All of the experiments were done in triplicate and twice. The statistical analyses for the IC₅₀ values have been conducted by SPSS 26.0.

2.5. Western Blot Assay for P-glycoprotein Expression

MCF-7/Dox cells were seeded at a density of 2×10⁵ cells/well in 6-well plates and incubated for 24 h. Experimental grouping and processing were the same as those discussed in the MDR Reversal Activity Assays section. After incubation for 48 h, cells were washed three times with PBS and lysed directly in the RIPA (Radio Immunoprecipitation Assay) buffer. The lysates were centrifuged at 12,000 rpm for 5 minutes, and the supernatants were collected. Supernatant protein concentrations were determined using a BCA protein assay kit. SDS-PAGE was used to separate whole cell lysates having equivalent amounts of protein to be transferred to polyvinylidene difluoride (PVDF) membranes. PVDF membranes were incubated with primary antibodies and then with HRP-conjugated secondary antibodies. The proteins were then detected using the ECL detection kit.

3. Results and Discussion

3.1. Structure Determination of Isolated Compounds

Compound **1** was isolated as a colorless oil and deduced to have a molecular formula of C₂₈H₅₁NO₆ by HR-ESIMS at *m/z* 520.3611 [M + Na]⁺ (calculated for C₂₈H₅₁NO₆Na, 520.3614), implying the presence of four degrees of unsaturation. The IR absorption bands at 3427, 1736, and 1641 cm⁻¹ implied the presence of hydroxy, ester carbonyl moieties, and double bonds, respectively. The ¹³C NMR (Table 1) data in combination with DEPT spectra displayed two ester groups at δ_C 171.8 (C-4'') and 175.4 (C-1'), an unbranched alkyl chain with two unsaturations at δ_C 14.4 (C-18'), 23.6 (C-17'), 26.0 (C-3'), 26.5 (C-11'), 28.1 (C-8', and C-14'), 30.2~30.7 (C-4', C-5', C-6', C-7', and C-15'), 32.7 (C-16'), 34.9 (C-2'), 129.0 (C-12'), 129.1 (C-10'), 130.9 (C-9'), 130.9 (C-13'), and five heteroatomic carbon signals at δ_C 66.5 (C-1), 68.5 (C-1''), 69.5 (C-2), 73.3 (C-3), 77.6 (C-3''), and three heteroatom methyl groups at δ_C 52.3 (3''-NCH₃ and 4''-OCH₃), and one methylene carbon at δ_C 29.0 (C-2''). An inspection of the ¹H NMR (Table 1) and HSQC spectra indicated one alkyl chain at δ_H 0.90 (3H, t, *J*=6.9 Hz, H-18'), 1.28~1.32 (14H, m, H-4'-7', H-15'-17'), 1.61 (2H, m, H-3'), 2.06 (4H, m, H-8', and H-14'), 2.35 (2H, t, *J*=7.5 Hz, H-2'), 2.77 (2H, t, *J*=6.4 Hz, H-11'), 5.31~5.34 (4H, m, H-10', H-12', H-9', and H-13'), eight heteroatomic hydrogen signals at δ_H 3.49 (2H, dd, *J*=13.3, 5.2 Hz, H-3), 3.53 (1H, td, *J*=12.6, 4.1 Hz, H-1''β), 3.65 (1H, m, H-1''α), 3.75 (1H, dd, *J*=11.4, 2.7 Hz, H-3''), 3.94 (1H, m, H-2), 4.06 (1H, dd, *J*=11.4, 6.3 Hz, H-1α), 4.16 (1H, dd, *J*=11.4, 4.4 Hz, H-1β), a methylene signals at δ_H 2.22 (1H, m, H-2''α), 2.06 (1H, m, H-2''β), and three methyl groups at δ_H 3.20 (9H, s).

According to the HMBC correlations from H-1 to C-1', C-2, and C-3, from H-2 to C-1 and C-3, from H-3 to C-1 and C-1'', the presence of glycerol moiety is suggested. The HMBC correlations from

H-1 to C-1' indicated the acylation of this glycerol methylene at position C-1. In the ^1H NMR spectrum, a strong singlet signal corresponding to the two equivalent methyl groups at δ_{H} 3.20 ppm correlates with HSQC at δ_{C} 52.3 ppm, indicating the presence of a dimethylammonium group. In-depth analysis of the 2D NMR data including additional ^1H - ^1H COSY and HMBC spectra led to the identification of a dimethylhomoserine unit with ^{13}C NMR signals at δ_{C} 68.5 (C-1''), 29.0 (C-2''), 77.6 (C-3''), 171.6 (C-4''), and 52.3 (3''-NCH₃). Which was also confirmed by the HMBC correlations from H-1'' β to C-3, C-2'' and C-3'', from H-2'' α to C-1'', C-3'' and C-4'', from H-3'' to C-1'', C-2'', C-4'' and 3''-NCH₃. The HMBC correlations from H-1'' β to C-3 suggested that the homoserine unit was attached to the glycerol moiety at C-3 via an ether bond. Based on ^1H - ^1H COSY correlations (H-17'/H-18', H-8'/H-9'/H-10'/H-11'/H-12'/H-13'/H-14') and key HMBC correlations (H-2' to C-1', C-3', C-4'; H-8' to C-6', C-7', C-9', C-10'; H-18' to C-16', C-17'), an unbranched alkyl chain with unsaturation was deduced. In the HMBC spectrum, the correlations from H-2' to C-1' and C-3' indicated that the carbonyl connected to an unbranched alkyl chain with two unsaturation. In Figure S8 the EI-MS spectrum of compound **1** presented fragment ions (at m/z 438, 262, and 117). The fragment ions at m/z 262, suggested that there is a linoleic acid moiety (Figure S9). Therefore, the structure of compound **1** is elucidated as shown in Figure 2. Thus, compound **1** was assigned as 9',12'-Octadecadienoic acid (9'Z,12'Z)-,3-[3''-(dimethylamino)-4''-methoxy-4''-oxobutoxy]-2-hydroxypropyl ester.

Table 1. ^1H NMR and ^{13}C NMR data of compound **1** in CD₃OD

Position	$\delta_{\text{C}}^{\text{a}}$ (δ in ppm)	$\delta_{\text{H}}^{\text{b}}$ (J in Hz)
1 β	66.5	4.16 (1H, dd, 11.4, 4.4)
1 α		4.06 (1H, dd, 11.4, 6.3)
2	69.5	3.94 (1H, m)
3	73.3	3.49 (2H, dd, 13.3, 5.2)
1'' β	68.5	3.53 (1H, td, 12.6, 4.1)
1'' α		3.65 (1H, m)
2'' α	29.0	2.22 (1H, m)
2'' β		2.06 (1H, m)
3''	77.6	3.75 (1H, dd, 11.4, 2.7)
4''	171.8	
3''-NCH ₃	52.3	3.20 (6H, s)
4''-OCH ₃	52.3	3.20 (3H, s)
1'	175.4	
2'	34.9	2.35 (2H, t, 7.5)
3'	26.0	1.61 (2H, m)
4'-7'	30.2-30.7	1.28-1.32 (8H, m)
8', 14'	28.1	2.06 (4H, m)
9', 13'	130.9	5.34 (2H, m)
10'	129.1	5.31 (1H, m)
11'	26.5	2.77 (2H, t, 6.4)
12'	129.0	5.31 (1H, m)
15'	30.2-30.7	1.28-1.32 (2H, m)
16'	32.7	1.28-1.32 (2H, m)
17'	23.6	1.28-1.32 (2H, m)
18'	14.4	0.90 (3H, t, 6.9)

^a Measured at 125 MHz. ^b Measured at 500 MHz.

Compound **2** was isolated as a yellow oil and the molecular formula was determined as C₁₉H₃₄O₄ by HR-ESIMS (*m/z* 349.2349 [M + Na]⁺), which corresponds to three degrees of unsaturation. The IR spectrum displayed absorption peaks at 3443, 1740 and 1633 cm⁻¹, indicating the presence of hydroxy groups, carbonyl moieties and double bonds. The ¹H NMR (Table 2) and DEPT spectra of Rubracin H indicated the presence of two olefinic protons [δ_{H} 5.80 (1H, m, H-3) and 5.73 (1H, m, H-4)], a methyl group [δ_{H} 0.89 (3H, t, *J* = 7.0 Hz, H-4')], a methoxy group [δ_{H} 3.60 (3H, s, H-7''-OMe)], three oxygenated methine groups [δ_{H} 4.11 (1H, dd, *J* = 5.9, 4.8 Hz, H-1), 3.48 (1H, m, H-5) and 3.39 (1H, m, H-7)] and 11 methylene groups [δ_{H} 1.87, 2.09 (2H, m, H-2), δ_{H} 1.49 (2H, m, H-6), δ_{H} 1.51 (2H, m, H-1'), δ_{H} 1.30 (2H, m, H-2''), δ_{H} 1.33 (2H, m, H-3''), δ_{H} 1.61, 1.43 (2H, m, H-1''), δ_{H} 1.37 (2H, m, H-2''), δ_{H} 1.35 (2H, m, H-3''), δ_{H} 1.32 (2H, m, H-4''), δ_{H} 1.58 (2H, m, H-5'') and δ_{H} 2.29 (2H, t, *J* = 7.5 Hz, H-6'')]. Analysis of the ¹³C NMR, DEPT and HSQC spectral data of **2** revealed the presence of 19 carbons, consisting of a carbonyl carbon [δ_{C} 174.1 (C-7'')], three oxygenated carbons [δ_{C} 73.6 (C-1), 70.7 (C-5) and 73.8 (C-7)], a methoxy group [δ_{C} 51.4 (C-7''-OMe)], a methyl group [δ_{C} 14.4 (C-4')], two olefinic carbons [δ_{C} 124.5 (C-3) and δ_{C} 130.8 (C-4)], 11 methylene carbons [δ_{C} 27.3 (C-2), 33.5 (C-6), 26.7 (C-1'), 32.7 (C-2'), 23.3 (C-3'), 34.2 (C-1''), 26.2 (C-2''), 29.9 (C-3''), 29.7 (C-4''), 25.6 (C-5'') and 34.2 (C-6'')]. Besides a carbonyl and a double bond, the remaining one unsaturation degree should be due to a ring.

Table 2. ¹H NMR and ¹³C NMR data of compound **2** in CD₃COCD₃

No.	$\delta_{\text{C}}^{\text{a}}$ (δ in ppm)	$\delta_{\text{H}}^{\text{b}}$ (<i>J</i> in Hz)
1	73.6	4.11 (1H, dd, 5.9, 4.8)
2 α	27.3	1.87 (1H, m)
2 β		2.09 (1H, m)
3	124.5	5.80 (1H, m)
4	130.8	5.73 (1H, m)
5	70.7	3.48 (1H, m)
6	33.5	1.49 (2H, m)
7	73.8	3.39 (1H, m)
1'	26.7	1.51 (2H, m)
2'	32.7	1.30 (2H, m)
3'	23.3	1.33 (2H, m)
4'	14.4	0.89 (3H, t, 7.0)
1'' β	34.2	1.43 (1H, m)
1'' α		1.61 (1H, m)
2''	26.2	1.37 (2H, m)
3''	29.9	1.35 (2H, m)
4''	29.7	1.32 (2H, m)
5''	25.6	1.58 (2H, m)
6''	34.2	2.29 (2H, t, 7.5)
7''	174.1	
7''-OMe	51.4	3.60 (3H, s)
5-OH		3.20, d, (5.2)

^a Measured at 125 MHz. ^b Measured at 500 MHz.

Compound **2** was suggested to have an alkyl chain connected to C-1, which is supported by HMBC correlations from H-4' to C-3' and C-2', from H-3' to C-2' and from H-1' to C-3', C-1 and C-2 and ¹H-¹H COSY correlations of H-1'/H-2' and H-1/H-2/H-3. The HMBC correlation from methoxy proton (H-7''-OMe) to carbonyl carbon (C-7'') confirmed the location of the methoxy group at C-7''. The existence of a fatty acid ester in **2** was unambiguously confirmed by HMBC correlations from H-1'' α to C-2'' and C-3'', from H-2'' to C-7 and C-4'', from H-3'' to C-2'' and C-4'', from H-5'' to C-3'', C-4'' and C-7'' and from H-6'' to C-4'', C-5'' and C-7'' and ¹H-¹H COSY correlations of H-7/H-1'' β and H-4''/H-5''/H-6''. The hydroxy group was located at C-5, as confirmed by the HMBC correlations from OH-5 to C-5 and C-6. The HMBC correlations of H-7 to C-5 and C-6, H-6 to C-5, C-7 and C-1'' and H-5 to C-6 and C-7, as well as the ¹H-¹H COSY correlations of H-1/H-2/H-3/H-4/H-5 and H-7/H-1'', formed an eight-membered ring by C-1, C-2, C-3, C-4, C-5, C-6 and C-7. The ROESY correlations of H-3 with H-

4 verified that these protons were placed on the same side. The significant ROESY correlations of H-5 with H-7 and of H-1 with H-5 and H-7 suggested that there were two possible isomers [(1R, 5R, 7R) and (1S, 5S, 7S)] of compound **2**. The experimental ECD spectrum of **2** was compared with the theoretical computation of the ECD spectrum using the time-dependent density functional theory (TD-DFT) approach to confirm the absolute configuration of **2**. As a result, as shown in Figure 3, the calculated ECD spectra of **2** were consistent with the experimental ECD results, indicating that the absolute configurations of **2** are presented as 1S, 5S and 7S. So, the absolute configuration of **2** was assigned as 1S, 5S and 7S. Thus, compound **2** was assigned as methyl ((1S,5S,7S, Z)-1-butyl-5-hydroxy-1,2,5,6-tetrahydro-2H-oxocin-2-yl) heptanoate.

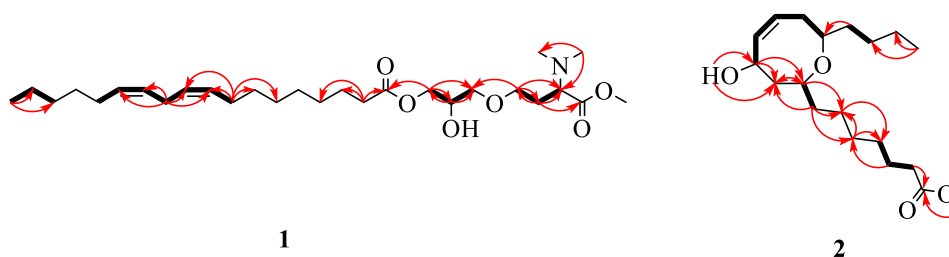


Figure 2. Key HMBC and ^1H - ^1H COSY correlations for compounds **1** and **2**

The structures of known compounds **3-8** were identified by comparison of their spectroscopic data with those in the literature and their structures were identified as Acetanilide (**3**) [27], N-(2-hydroxyphenyl) acetamide (**4**) [28], thymidine (**5**) [29], 2'-deoxyuridine (**6**) [29], uridine (**7**) [30] and adenosine (**8**) [30].

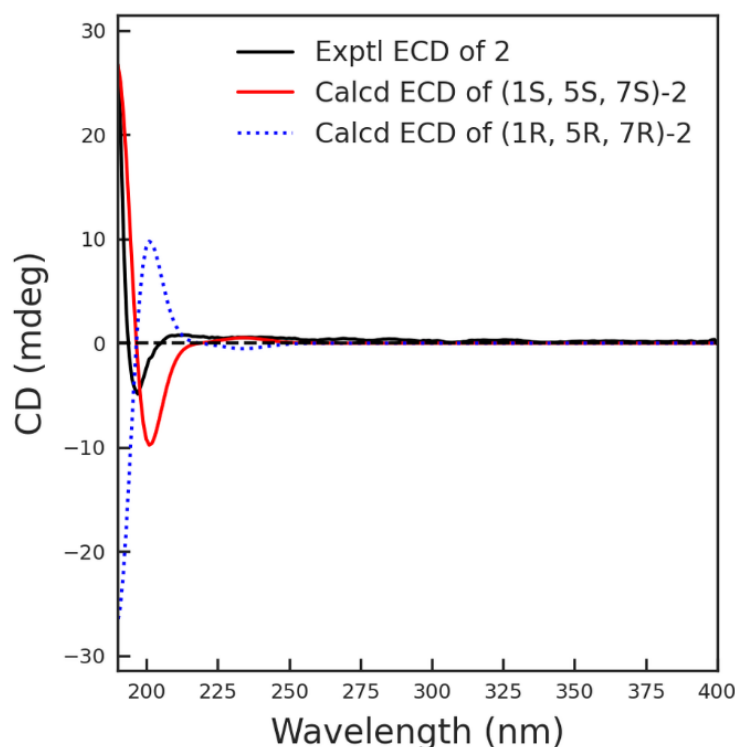


Figure 3. Experimental and calculated ECD spectra of **2**.

3.2 Effect of Compound 1 on Reversing MDR In Vitro

Table S1 shows the comparison data of the cytotoxicity of doxorubicin against the sensitive (MCF-7, A549 and K562 cells) and MDR tumor cell lines (MCF-7/Dox, A549/Dox and K562/Dox cells), which indicated that the latter cells were drug-resistant. We found that compound **1** showed no evident cytotoxic effects on MDR tumor cell lines at concentrations below 25 $\mu\text{g/mL}$ for up to 48 hours of treatment (Figure S13), individually, using CCK-8 assays. On the other hand, doxorubicin with and without compound **1** was used to treat MDR tumor cell lines for 48 h. As a result of those assays in drug-resistant K562/Dox cells, the treatment of doxorubicin with 10 $\mu\text{g/mL}$ concentration of compound **1** enhanced chemosensitivity of the MDR cells to doxorubicin (Table 3) were observed in all the three drug-resistant cell lines, viz MCF-7/Dox, A549/Dox and K562/Dox and by the treatments of doxorubicin with 20 $\mu\text{g/mL}$ concentration of compound **1** resulted in a significant increase in the cytotoxicity of doxorubicin, of which the IC_{50} values dropped drastically from 102.762 ± 0.953 to 59.411 ± 2.230 , from 3.330 ± 0.327 to 2.387 ± 0.081 and from 5.053 ± 0.226 to 3.790 ± 0.284 $\mu\text{g/mL}$, respectively.

Table 3. Cytotoxicity of sole doxorubicin and in combination with compound **1** (PF29) or Verapamil (VRP) in doxorubicin-resistant cell lines in vitro.

Drug	$\text{IC}_{50} \pm \text{SD}^{\text{a}}$ ($\mu\text{g/mL}$)		
	MCF-7/Dox	A549/Dox	K562/Dox
Doxorubicin	102.762 ± 0.953	3.330 ± 0.327	5.053 ± 0.226
+ 5 $\mu\text{g/mL}$ PF29	135.878 ± 2.021	3.146 ± 0.309	4.802 ± 0.163
+ 10 $\mu\text{g/mL}$ PF29	116.122 ± 1.856	2.772 ± 0.096	$4.351 \pm 0.329^*$
+ 20 $\mu\text{g/mL}$ PF29	$59.411 \pm 2.230^{***}$	$2.387 \pm 0.081^{**}$	$3.790 \pm 0.284^{**}$
+ 5 $\mu\text{g/mL}$ VRP	53.365 ± 2.210	2.414 ± 0.263	3.820 ± 0.832
+ 10 $\mu\text{g/mL}$ VRP	39.626 ± 2.134	1.544 ± 0.065	3.016 ± 0.512
+ 20 $\mu\text{g/mL}$ VRP	29.543 ± 1.326	1.336 ± 0.115	1.842 ± 0.215

^a Cells were exposed to various concentrations of Dox, with or without 5, 10, and 20 $\mu\text{g/mL}$ compound **1** (PF29) or Verapamil (VRP) for 48 h. IC_{50} values were determined by regression analyses and expressed as means \pm SD of three replicates.

Finally, we tested the P-gp expression in MCF-7/Dox cells treated with doxorubicin and compound **1** for 48 h. Western blot assays showed that the test with 20 $\mu\text{g/mL}$ concentration of compound **1** had a significant suppression effect on the expression level of P-gp (Figure 4), which indicated that compound **1** reversed the MDR of the three drug-resistant cell lines and, a patent application was also done by our team for the **1**.

In conclusion, two new compounds named Rubracin A and H, and six known compounds (**3-8**) were isolated from *T. rubra* fungus. These new compounds were isolated from the nature for the first time. In addition, we also isolated analogs from *T. rubra* with one more ester chain than compound **1**, which could be the hydrolysis product of the analog. However, we analyzed the chemical composition of the EtOAc extract by UHPLC-MS. Compared with high-precision mass spectrometry, which shows that compound **1** is the metabolite of *T. rubra*, not the hydrolysis product of the analog. MDR reversal activity assays indicated that compound **1** reversed the MDR. As a Pgp modulator, compound **1** reversed Pgp-MDR by suppressing Pgp expression. Although the activity of compound **1** is weaker than that of verapamil, it provides a reference for enriching the database of lead compounds for P-gp inhibitors.

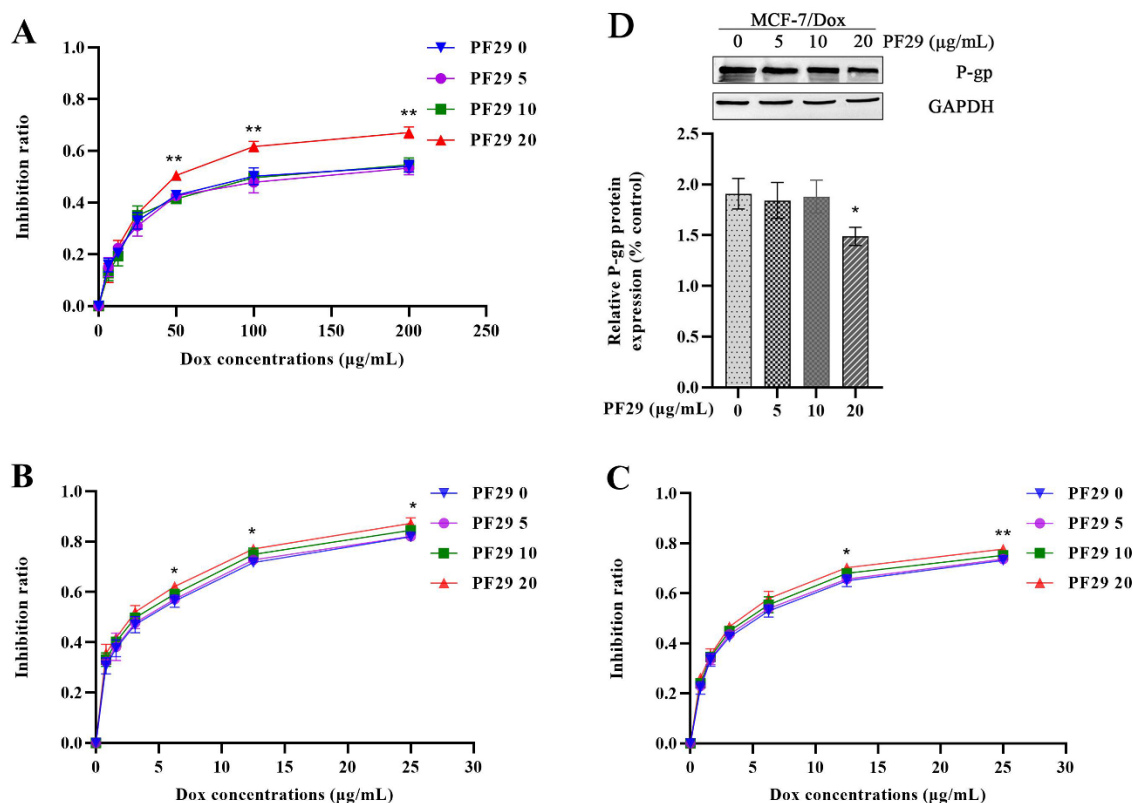


Figure 4. Effects of compound **1** on viability and Pgp expression of Dox-treated MDR cancer cells. Cells were exposed to various concentrations of Dox, with and without 5, 10 and 20 μg/mL compound **1** (PF29) for 48 h in (A) MCF-7/Dox cells, (B) A549/Dox and (C) K562/Dox cells. (D) Suppression effect of compound **1** on P-gp expression. A representative result is shown from three independent experiments.

Acknowledgments

This study was supported by the National Natural Science Foundation of China (NSFC No.31670027, 32170019, 32160667, and 31901947) and the Open Fund Program of Engineering and Research Center for Southwest Bio-Pharmaceutical Resources of National Education Ministry of China, Guizhou University. No. GZUKEY20160.

Supporting Information

Supporting information accompanies this paper on <http://www.acgpubs.org/journal/records-of-natural-products>

ORCID

Xuebo Zeng: [0000-0001-8517-0049](https://orcid.org/0000-0001-8517-0049)

Shengyan Qian: [0000-0002-1239-4516](https://orcid.org/0000-0002-1239-4516)

Yongzhong Lu: [0000-0002-1033-5782](https://orcid.org/0000-0002-1033-5782)

Yongjie Li: [0000-0002-3334-8922](https://orcid.org/0000-0002-3334-8922)

Lizhuang Chen: [0000-0002-1490-7776](https://orcid.org/0000-0002-1490-7776)

Yixin Qian: [0000-0002-4145-1807](https://orcid.org/0000-0002-4145-1807)

Zhangjiang He: [0000-0002-7120-1227](https://orcid.org/0000-0002-7120-1227)

Jichuan Kang: [0000-0002-6294-5793](https://orcid.org/0000-0002-6294-5793)

References

- [1] R. L. Siegel, K. D. Miller, H. E. Fuchs and A. Jemal (2022). Cancer statistics, *Cancer J. Clin.* **72**, 7-33.
- [2] W. Chen, R. Zheng, P. D. Baade, S. Zhang, H. Zeng and F. Bray (2016). Cancer statistics in China, 2015, *CA Cancer J. Clin.* **66**, 115-132.
- [3] L. Han, Y. Wang, X. Guo, Y. Zhou, J. Zhang and N. Wang (2014). Downregulation of MDR1 gene by cepharanthine hydrochloride is related to the activation of c-Jun/JNK in K562/ADR cells, *BioMed Res. Int.* **2014**, 1-6.
- [4] D. Szabo, G. S. Jr, I. Ocsovszki, A. Aszalos and J. Molnar (1999). Anti-psychotic drugs reverse multidrug resistance of tumor cell lines and human AML cells ex-vivo, *Cancer Lett.* **139**, 115-119.
- [5] R. W. Robey, K. M. Pluchino, M. D. Hall, A. T. Fojo, S. E. Bates and M. M. Gottesman (2018). Revisiting the role of ABC transporters in multidrug-resistant cancer, *Nat Rev Cancer.* **18**, 452-464.
- [6] F. X. Mahon, F. Belloc, V. Lagarde, C. Chollet, F. Moreau-Gaudry and J. Reiffers (2003). MDR1 gene overexpression confers resistance to imatinib mesylate in leukemia cell line models, *Blood* **101**, 2368-2373.
- [7] N. Gao, Z. C. Shang, P. Yu, J. Luo, K. L. Jian and L. Y. Kong (2017). Alkaloids from the endophytic fungus *Penicillium brefeldianum* and their cytotoxic activities, *Chinese Chem. Lett.* **28**, 1194-1199.
- [8] X. Xie, S. Lu, X. Pan, M. Zou, F. Li and H. Lin (2021). Antiviral bafilomycins from a feces-inhabiting *Streptomyces* sp, *J. Nat. Prod.* **84**, 537-543.
- [9] M. H. Hsieh, G. Hsiao, C. H. Chang, Y. L. Yang, Y. M. Ju and Y. H. Kuo (2021). Polyketides with anti-neuroinflammatory activity from *Theissenia cinerea*, *J. Nat. Prod.* **84**, 1898-1903.
- [10] G. Chen, Z. Jiang, J. Bai, H. Wang, S. Zhang and Y. H. Pei (2015), Isolation, structure determination, in vivo/vitro assay and docking study of a xanthone with antitumor activity from fungus *Penicillium oxalicum*, *Rec. Nat. Prod.* **9**, 184-189.
- [11] S. Shi, Y. Li, Y. Ming, C. Li, Z. Li, J. Chen and M. Luo (2018). Biological Activity and Chemical Composition of the Endophytic Fungus *Fusarium* sp. TP-G1 Obtained from the Root of *Dendrobium officinale* Kimura et Migo, *Records of Natural Products* **12**, 549-556.
- [12] S. S. Yang, M. J. Cheng, H. Y. Chan, S. Y. Hsieh, H. C. Wu and G. F. Yuan (2017). New secondary metabolites from an endophytic fungus in *Porodaedalea pini*, *Rec. Nat. Prod.* **11**, 251-257.
- [13] A. Stierle, G. Strobel and D. Stierle (1993). Taxol and taxane production by *taxomyces andreanae*, an endophytic fungus of pacific yew, *Science* **260**, 214-216.
- [14] N. Zhang, C. Zhang, X. Xiao, Q. Zhang and B. Huang (2016). New cytotoxic compounds of endophytic fungus *Alternaria* sp. isolated from *Broussonetia papyrifera* (L.) Vent, *Fitoterapia* **110**, 173-180.
- [15] M. M. Zhai, F. M. Qi, J. Li, C. X. Jiang, Y. Hou and Y. P. Shi (2016). Isolation of secondary metabolites from the soil-derived fungus *Clonostachys rosea* YRS-06, a biological control agent, and evaluation of antibacterial activity, *J. Agric. Food Chem.* **64**, 2298-2306.
- [16] Y. Z. Lu, J. K. Liu, K. D. Hyde, R. Jeewon, J. C. Kang and C. Fan, (2018). A taxonomic reassessment of Tubeufiales based on multi-locus phylogeny and morphology, *Fungal Divers.* **92**, 131-344.
- [17] L. Muggia, C. Gueidan, K. Knudsen, G. Perlmutter and M. Grube (2012). The lichen connections of black fungi, *Mycopathologia* **175**, 523-535.
- [18] I. Bardarov, M. Mitov, D. Ivanova and Y. Hubenova (2018). Light-dependent processes on the cathode enhance the electrical outputs of sediment microbial fuel cells, *Bioelectrochemistry* **122**, 1-10.
- [19] T. Julia, W. Bernd, T. Michael, D. Rolf, T. Teja, E. Anne, and S. Christoph (2016). Trophic and non-trophic interactions in a biodiversity experiment assessed by next-generation sequencing, *Plos One* **11**, e0148781.
- [20] C. L. Schoch, G. H. Sung, F. L. Giráldez, J. P. Townsend and J. Miadlikowska (2009). The ascomycota tree of life: A phylum-wide phylogeny clarifies the origin and evolution of fundamental reproductive and ecological traits, *System. Biol.* **58**, 224-239.
- [21] P. Jiao, J. B. Gloer, J. Campbell and C. A. Shearer (2006). Altenuene derivatives from an unidentified freshwater fungus in the family Tubeufiaceae, *J. Nat. Prod.* **69**, 612-615.
- [22] H. Hu, H. Guo, E. Li, X. Liu, Y. Zhou and Y. Che (2006). Decaspiroenes F-I, bioactive secondary metabolites from the saprophytic fungus *Helicoma wiridis*, *J. Nat. Prod.* **69**, 1672-1675.
- [23] H. Itazaki, K. Nagashima, K. Sugita, H. Yoshida, Y. Kawamura and Y. Yasuda (1990). Isolation and structural elucidation of new cyclotetrapeptides, trapoxins A and B, having detransformation activities as antitumor agent, *J. Antibiot.* **43**, 1524-1532.
- [24] Y. Ohtsu, H. Sasamura, T. Shibata, H. Nakajima, M. Hino and T. Fujii (2003). The novel gluconeogenesis inhibitors FR225659 and related compounds that originate from *Helicomyces* sp. No. 19353 II. Biological profiles, *J. Antibiot.* **56**, 689-693.

- [25] L. Z. Chen, Y. X. Qian, J. C. Kang, L. Wang, Y. Z. Lu and C. Fan (2020). The reversal bioactivities of multidrug resistance of MCF-7/ADM cells induced by two *Tubeufia* fungal strains, *Mycosystema* **39**, 817-826.
- [26] H. Tominaga, M. Ishiyama, F. Ohseto, K. Sasamoto, T. Hamamoto, K. Suzukic and M. Watanabe (1999). A water-soluble tetrazolium salt useful for colorimetric cell viability assay, *Anal. Commun.* **36**, 47-50.
- [27] M. H. Tao, D. L. Li, W. M. Zhang, J. W. Tan and X. Y. Wei (2011). Study on the chemical constituents of endophytic fungus *Fimetariella rabenhorstii* isolated from *Aquilaria sinensis*, *J. Chin. Medicin. Mater.* **34**, 221-223.
- [28] Z. Shang, X. Li, L. Meng, C. Li, S. Gao and C. Huang (2012). Chemical profile of the secondary metabolites produced by a deep-sea sediment-derived fungus *Penicillium commune* SD-118*, *Chin. J. Ocean. Limnol.* **30**, 305-314.
- [29] D. T. A. Youssef, J. M. Badr, L. A. Shaala, G. A. Mohamed and F. H. Bamanie (2015). Ehrenasterol and biemnic acid; new bioactive compounds from the Red Sea sponge *Biemna ehrenbergi*, *Phytochemistry Letters* **12**, 296-301.
- [30] Y. T. Ma, L. R. Qiao, W. Q. Shi, A. L. Zhang and J. M. Gao (2010). Metabolites produced by an endophyte *Alternaria alternata* isolated from *Maytenus hookeri*, *Chem. Nat. Compound.* **46**, 504-506.

A C G
publications

© 2022 ACG Publications